The reaction dynamics of the $^{16}O(e,e'p)$ cross section at high missing energies

N. Liyanage,[17] B. D. Anderson,[13] K. A. Aniol,[2] L. Auerbach,[29] F. T. Baker,[7] J. Berthot,[1] W. Bertozzi,[17] P. -Y. Bertin,[1] L. Bimbot,[22] W. U. Boeglin,[5] E. J. Brash,[24] V. Breton,[1] H. Breuer,[16] E. Burtin,[26] J. R. Calarco,[18] L. Cardman,[30] G. D. Cates,[23] C. Cavata,[26] C. C. Chang,[16] J. -P. Chen,[30] E. Cisbani,[12] D. S. Dale,[14] R. De Leo,[10] A. Deur,[1] B. Diederich,[21] P. Djawotho,[33] J. Domingo,[30] B. Doyle,[14] J. -E. Ducret,[26] M. B. Epstein,[2] L. A. Ewell,[16] J. M. Finn,[33] K. G. Fissum,[17] H. Fonvieille,[1] B. Frois,[26] S. Frullani,[12] J. Gao,[17] F. Garibaldi,[12] A. Gasparian,[8,14] S. Gilad,[17] R. Gilman,[25,30] A. Glamazdin,[15] C. Glashausser,[25] J. Gomez,[30] V. Gorbenko,[15] T. Gorringe,[14] F. W. Hersman,[18] R. Holmes,[28] M. Holtrop,[18] N. d'Hose,[26] C. Howell,[4] G. M. Huber,[24] C. E. Hyde-Wright,[21] M. Iodice,[12] C. W. de Jager,[30] S. Jaminion,[1] M. K. Jones,[33] K. Joo,[32] C. Jutier,[1,21] W. Kahl,[28] S. Kato,[34] J. J. Kelly,[16] S. Kerhoas,[26] M. Khandaker,[19] M. Khayat,[13] K. Kino,[31] W. Korsch,[14] L. Kramer,[5] K. S. Kumar,[23] G. Kumbartzki,[25] G. Laveissière,[1] A. Leone,[11] J. J. LeRose,[30] L. Levchuk,[15] M. Liang,[30] R. A. Lindgren,[32] G. J. Lolos,[24] R. W. Lourie,[27] R. Madey,[8,13,30] K. Maeda,[31] S. Malov,[25] D. M. Manley,[13] D. J. Margaziotis[2] P. Markowitz,[5] J. Martino,[26] J. S. McCarthy,[32] K. McCormick,[21] J. McIntyre,[25] R. L. J. van der Meer,[24] Z. -E. Meziani,[29] R. Michaels,[30] J. Mougey,[3] S. Nanda,[30] D. Neyret,[26] E. A. J. M. Offermann,[30] Z. Papandreou,[24] C. F. Perdrisat,[33] R. Perrino,[11] G. G. Petratos,[13] S. Platchkov,[26] R. Pomatsalyuk,[15] D. L. Prout,[13] V. A. Punjabi,[19] T. Pussieux,[26] G. Quéméner,[33] R. D. Ransome,[25] O. Ravel,[1] Y. Roblin,[1] R. Roche,[6] D. Rowntree,[17] G.A. Rutledge,[33] P. M. Rutt,[30] A. Saha,[30] T. Saito,[31] A. J. Sarty,[6] A. Serdarevic-Offermann,[24] T. P. Smith,[18] A. Soldi,[20] P. Sorokin,[15] P. Souder,[28] R. Suleiman,[13] J. A. Templon,[7] T. Terasawa,[31] L. Todor,[21] H. Tsubota,[31] H. Ueno,[34] P. E. Ulmer,[21] G.M. Urciuoli,[12] P. Vernin,[26] S. van Verst,[17] B. Vlahovic,[20,30] H. Voskanyan,[35] J. W. Watson,[13] L. B. Weinstein,[21] K. Wijesooriya,[33] R. Wilson,[9] B. Wojtsekhowski,[30] D. G. Zainea,[24] V. Zeps,[14] J. Zhao,[17] Z. -L. Zhou[17]

(The Jefferson Lab Hall A Collaboration)

[1] *Université Blaise Pascal/IN2P3, F-63177 Aubière, France*
[2] *California State University, Los Angeles, California 90032, USA*
[3] *Institut des Sciences Nucléaires, F-38026 Grenoble, France*
[4] *Duke University, Durham, North Carolina 27706, USA*
[5] *Florida International University, Miami, Florida 33199, USA*
[6] *Florida State University, Tallahassee, Florida 32306, USA*
[7] *University of Georgia, Athens, Georgia 30602, USA*
[8] *Hampton University, Hampton, Virginia 23668, USA*
[9] *Harvard University, Cambridge, Massachusetts 02138, USA*
[10] *INFN, Sezione di Bari and University of Bari, I-70126 Bari, Italy*
[11] *INFN, Sezione di Lecce, I-73100 Lecce, Italy*
[12] *INFN, Sezione Sanitá and Istituto Superiore di Sanitá, Laboratorio di Fisica, I-00161 Rome, Italy*
[13] *Kent State University, Kent, Ohio 44242, USA*
[14] *University of Kentucky, Lexington, Kentucky 40506, USA*
[15] *Kharkov Institute of Physics and Technology, Kharkov 310108, Ukraine*
[16] *University of Maryland, College Park, Maryland 20742, USA*
[17] *Massachusetts Institute of Technology, Cambridge, Massachusetts 02139, USA*
[18] *University of New Hampshire, Durham, New Hampshire 03824, USA*
[19] *Norfolk State University, Norfolk, Virginia 23504, USA*
[20] *North Carolina Central University, Durham, North Carolina 27707, USA*
[21] *Old Dominion University, Norfolk, Virginia 23529, USA*
[22] *Institut de Physique Nucléaire, F-91406 Orsay, France*
[23] *Princeton University, Princeton, New Jersey 08544, USA*
[24] *University of Regina, Regina, Saskatchewan, Canada, S4S 0A2*
[25] *Rutgers, The State University of New Jersey, Piscataway, New Jersey 08854, USA*
[26] *CEA Saclay, F-91191 Gif-sur-Yvette, France*
[27] *State University of New York at Stony Brook, Stony Brook, New York 11794, USA*
[28] *Syracuse University, Syracuse, New York 13244, USA*
[29] *Temple University, Philadelphia, Pennsylvania 19122, USA*
[30] *Thomas Jefferson National Accelerator Facility, Newport News, Virginia 23606, USA*
[31] *Tohoku University, Sendai 980, Japan*
[32] *University of Virginia, Charlottesville, Virginia 22901, USA*
[33] *College of William and Mary, Williamsburg, Virginia 23187, USA*
[34] *Yamagata University, Yamagata 990, Japan*
[35] *Yerevan Physics Institute, Yerevan 375036, Armenia*

(August 30, 2000)

We measured the cross section and response functions (R_L, R_T, and R_{LT}) for the ^{16}O$(e,e'p)$ reaction in quasielastic kinematics for missing energies $25 \leq E_{\rm miss} \leq 120$ MeV at various missing momenta $P_{\rm miss} \leq 340$ MeV/c. For $25 < E_{\rm miss} < 50$ MeV and $P_{\rm miss} \approx 60$ MeV/c, the reaction is dominated by single-nucleon knockout from the $1s_{1/2}$-state. At larger $P_{\rm miss}$, the single-particle aspects are increasingly masked by more complicated processes. For $E_{\rm miss} > 60$ MeV and $P_{\rm miss} > 200$ MeV/c, the cross section is relatively constant. Calculations which include contributions from pion exchange currents, isobar currents and short-range correlations account for the shape and the transversity but only for half of the magnitude of the measured cross section.

PACS numbers: 25.30.Fj, 27.20.+n

The $(e,e'p)$ reaction in quasielastic kinematics ($\omega \approx Q^2/2m_p$)[1] has long been a useful tool for the study of nuclear structure. $(e,e'p)$ cross section measurements have provided both a wealth of information on the wave function of protons inside the nucleus and stringent tests of nuclear theories. Response function measurements have provided detailed information about the different reaction mechanisms contributing to the cross section.

In the first Born approximation, the unpolarized $(e,e'p)$ cross section can be separated into four independent response functions, R_L (longitudinal), R_T (transverse), R_{LT} (longitudinal-transverse), and R_{TT} (transverse-transverse) [1]. These response functions contain all the information that can be extracted from the hadronic system using the $(e,e'p)$ reaction.

Originally, the quasielastic cross section was attributed entirely to single-particle knockout from the valence states of the nucleus. However, a series of ^{12}C$(e,e'p)$ experiments performed at MIT-Bates [2–6] measured much larger cross sections at high missing energy than were expected by single-particle knockout models. ^{12}C$(e,e'p)$ response function data reported by Ulmer *et al.* [2] show a substantial increase in the transverse-longitudinal difference, $(S_T - S_L)$,[2] above the two-nucleon emission threshold. Similar R_T/R_L enhancement has also been observed by Lanen *et al.* for ^{6}Li [9], by van der Steenhoven *et al.* for ^{12}C [10] and, more recently, by Dutta *et al.* for ^{12}C, ^{56}Fe, and ^{197}Au [11].

There have been several theoretical attempts [12–14] to explain the continuum strength using two-body knockout models and final-state interactions, but no single model has been able to explain all the data.

In this first Jefferson Lab Hall A experiment [15], we studied the ^{16}O$(e,e'p)$ reaction in the quasielastic region at $Q^2 = 0.8$ (GeV/c)^2 and $\omega = 439$ MeV ($|\vec{q}| \approx 1$ GeV/c). We extracted the R_L, R_T, and R_{LT} response functions from cross sections measured at several beam energies, electron angles, and proton angles for $P_{\rm miss} \leq 340$ MeV/c. This paper reports the results for $E_{\rm miss} > 25$ MeV; p-shell knock-out region ($E_{\rm miss} < 20$ MeV) results from this experiment were reported in [16].

We scattered the $\sim$70 μA continuous electron beam from a waterfall target [17] with three foils, each $\sim$130 mg/cm^2 thick. We detected the scattered electrons and knocked-out protons in the two High Resolution Spectrometers (HRS$_e$ and HRS$_h$). The details of the Hall A experimental setup are given in [18,19].

We measured the ^{16}O$(e,e'p)$ cross section at three beam energies, keeping $|\vec{q}|$ and ω fixed in order to separate response functions and understand systematic uncertainties. Table I shows the experimental kinematics.

The accuracy of a response-function separation depends on precisely matching the values of $|\vec{q}|$ and ω for different kinematic settings. In order to match $|\vec{q}|$, we measured ^{1}H(e,ep) (also using the waterfall target) with a pinhole collimator in front of the HRS$_e$. The momentum of the detected protons was thus equal to $\vec{q}$. We determined the ^{1}H(e,ep) momentum peak to $\frac{\delta p}{p} = 1.5 \times 10^{-4}$, allowing us to match $\frac{\delta|\vec{q}|}{|\vec{q}|}$ to 1.5×10^{-4} between the different kinematic settings. Throughout the experiment, ^{1}H(e,e) data, measured simultaneously with ^{16}O$(e,e'p)$, provided a continuous monitor of both luminosity and beam energy.

The radiative corrections to the measured cross sections were performed by two independent methods; using the code RADCOR [19,20], which unfolds the radiative tails in $(E_{\rm miss}, P_{\rm miss})$ space, and using the code MCEEP [21] which simulates the radiative tail based on the prescription of Borie and Drechsel [22]. The corrected cross sections from the two methods agreed within the statistical uncertainties of these data. The radiative correction to the continuum cross section for $60 < E_{\rm miss} < 120$ MeV was about 10% of the measured cross section.

At $\theta_{pq} = \pm 8°$, R_{LT} extracted independently at beam energies of 1.643 GeV and 2.442 GeV agree well within statistical uncertainties. This indicates that the systematic uncertainties are smaller than the statistical uncertainties. The systematic uncertainty in cross section mea-

[1] The kinematical quantities are: the electron scattered at angle θ_e transfers momentum $\vec{q}$ and energy ω with $Q^2 = \vec{q}^{\,2} - \omega^2$. The ejected proton has mass m_p, momentum $\vec{p}_p$, energy E_p, and kinetic energy T_p. The cross section is typically measured as a function of missing energy $E_{\rm miss} = \omega - T_p - T_{\rm recoil}$ and missing momentum $P_{\rm miss} = |\vec{q} - \vec{p}_p|$. The polar angle between the ejected proton and virtual photon is θ_{pq} and the azimuthal angle is ϕ. $\theta_{pq} > 0°$ corresponds to $\phi = 180°$ and $\theta_p > \theta_q$. $\theta_{pq} < 0°$ corresponds to $\phi = 0°$.

[2] $S_X = \frac{\sigma_{\rm Mott} V_X R_X}{\sigma_X^{ep}}$, where X ϵ $\{T, L\}$, and σ_X^{ep} is calculated from the off-shell ep cross section obtained using deForest's cc1 prescription [7,8].

surements is about 5%. This uncertainty is dominated by the uncertainty in the ^{1}H(e,e) cross section to which the data were normalized [23].

Figure 1 shows the measured cross section as a function of missing energy at $E_{\rm beam} = 2.4$ GeV for various proton angles, $2.5° \leq \theta_{pq} \leq 20°$. The average missing momentum increases with θ_{pq} from 50 MeV/c to 340 MeV/c. The prominent peaks at 12 MeV and 18 MeV are due to 1p-shell proton knockout and are described in [16], where it was shown that the p-shell cross sections can be explained up to $P_{\rm miss} = 340$ MeV/c by relativistic Distorted Wave Impulse Approximation (DWIA) calculations. However the spectra for $E_{\rm miss} > 20$ MeV exhibit a very different behavior. At the lowest missing momentum, $P_{\rm miss} \approx 50$ MeV/c, the wide peak centered at $E_{\rm miss} \approx 40$ MeV is due predominantly to knockout of protons from the $1s_{1/2}$-state. This peak is less prominent at $P_{\rm miss} \approx 145$ MeV/c and has vanished beneath a flat background for $P_{\rm miss} \geq 200$ MeV/c. At $E_{\rm miss} > 60$ MeV or $P_{\rm miss} > 200$ MeV/c, the cross section does not depend on $E_{\rm miss}$ and decreases only weakly with $P_{\rm miss}$.

We compared our results to single-particle knockout calculations by Kelly [24] and Ryckebusch [25–27] to determine how much of the observed continuum ($E_{\rm miss} >$ 20 MeV) cross section can be explained by $1s_{1/2}$-state knockout. Kelly [24] performed DWIA calculations using a relativized Schrödinger equation in which the dynamical enhancement of lower components of Dirac spinors is represented by an effective current operator [28]. He used the NLSH bound-state wave function [29] and the energy dependent, atomic-mass independent optical potential EDAIO [30]. These calculations accurately describe the 1p-shell missing momentum distributions up to 340 MeV/c [16]. For the $1s_{1/2}$-state, Kelly used a normalization factor of 0.73 and spread the cross section and the response functions over missing energy using the Lorentzian parameterization of Mahaux [31]. At small $P_{\rm miss}$, where there is a clear peak at 40 MeV, this model describes the data well. At larger $P_{\rm miss}$, where there is no peak at 40 MeV, the DWIA cross section is much smaller than the measured cross section (see Figure 1). Relativistic DWIA calculations by other authors [32,33] show similar results. This confirms the attribution of the large missing momentum cross section to non-single-nucleon knockout.

Figure 1 also shows calculations by Ryckebusch *et al.* [25–27] using a non-relativistic single-nucleon knockout Hartree-Fock (HF) model which uses the same potential for both the ejectile and bound nucleons. Unlike DWIA, this approach conserves current at the one-body level, but it also requires much smaller normalization factors because it lacks a mechanism for diversion of flux from the single-nucleon knockout channel. At small missing momentum, this model describes both the p-shell and s-shell cross sections well. As the missing momentum increases, it progressively overestimates the p-shell and s-shell cross sections. The most important difference between the DWIA and HF single-nucleon knockout models is the absorptive potential; its omission from the HF model increases the HF cross section for $P_{\rm miss} \approx 300$ MeV/c by an order of magnitude for both p-shell and s-shell.

Figure 1 also shows $(e,e'pn)$ and $(e,e'pp)$ contributions to the $(e,e'p)$ cross section calculated by Ryckebusch *et al.* [34]. This calculation has also been performed in a HF framework. The cross section for the two particle knock-out has been calculated in the "spectator approximation" assuming that the two knocked-out nucleons will escape from the residual $A-2$ system without being subject to inelastic collisions with other nucleons. Then the two particle knock-out cross section has been integrated over the phase-space of the undetected particle to obtain the contribution to the $(e,e'p)$ cross section. This calculation includes contributions mediated by pion-exchange currents, intermediate Δ creation and central and tensor short-range correlations. According to this calculation, in our kinematics, two-body currents (pion-exchange and Δ) account for approximately 85% of the calculated $(e,e'pn)$ and $(e,e'pp)$ strength. Short-range tensor correlations contribute approximately 13% while short-range central correlations contribute only about 2%. Since the two-body current contributions are predominantly transverse, the calculated $(e,e'pn)$ and $(e,e'pp)$ cross section is mainly transverse in our kinematics. The flat cross section predicted by this calculation for $E_{\rm miss} > 50$ MeV is consistent with the data, but it accounts for only about half the measured cross section. Hence, additional contributions to the cross section such as heavier meson exchange and processes involving more than two hadrons must be considered.

Figures 2-4 present the separated response functions for various proton angles. Due to kinematic constraints, we were only able to separate the responses for $E_{\rm miss} < 60$ MeV. The separated response functions can be used to check the reaction mechanism. If the excess continuum strength at high $P_{\rm miss}$ is dominated by two body processes rather than by correlations, then it should be predominantly transverse.

Figure 2 presents the separated response functions for $\langle P_{\rm miss} \rangle \approx 60$ MeV/c. The wide peak centered around $E_{\rm miss} \approx 40$ MeV in both R_L and R_T corresponds primarily to single-particle knockout from the $1s_{1/2}$-state. The difference between the transverse and longitudinal spectral functions $(S_T - S_L)$, which is expected to be zero for a free nucleon, appears to increase slightly with $E_{\rm miss}$. The magnitude of $(S_T - S_L)$ measured here is consistent with the decrease in $(S_T - S_L)$ with Q^2 seen in the measurements of Ulmer *et al.* [2] at $Q^2 = 0.14$ (GeV/c)^2 and by Dutta *et al.* [11] at $Q^2 = 0.6$ and 1.8 (GeV/c)^2. This suggests that, in parallel kinematics, transverse non-single-nucleon knockout processes decrease with Q^2.

Figure 3 presents the separated response functions

(R_{L+TT}[3], R_T, and R_{LT}) for $|\theta_{pq}| = 8°$ ($\langle P_{\rm miss}\rangle \approx 145$ MeV/c). The Mahaux parameterization does not reproduce the shape of R_L or of R_T as a function of missing energy. For $E_{\rm miss} < 40$ MeV, all calculated response functions underestimate the data suggesting the excitation of states with a complex structure between the p- and s-shells. For $E_{\rm miss} > 50$ MeV, R_{L+TT} (which is mainly longitudinal because $\frac{V_{TT}}{V_L}R_{TT}$ is estimated to be only about 7% of R_L [24] in these kinematics) is consistent with both zero and with the calculations. R_T, on the other hand, remains nonzero to at least 60 MeV. R_T is also significantly larger than the DWIA calculation. R_{LT} is about twice as large as the DWIA calculation over the entire range of $E_{\rm miss}$. R_{LT} is nonzero for $E_{\rm miss} > 50$ MeV, indicating that R_L is also nonzero in that range.

Figure 4 presents the separated response functions for $|\theta_{pq}| = 16°$ ($\langle P_{\rm miss}\rangle \approx 280$ MeV/c). At this missing momentum, none of the measured response functions show a peak at $E_{\rm miss} \approx 40$ MeV where single-particle knockout from the $1s_{1/2}$-state is expected. R_{L+TT} is close to zero and the DWIA calculation. However, R_T and R_{LT} are much larger than the DWIA calculation. R_T is also much larger than R_{LT} indicating that the cross section is due in large part to transverse two-body currents. The fact that R_{LT} is nonzero indicates that R_L, although too small to measure directly, is also nonzero.

To summarize, we have measured the cross section and response functions (R_L, R_T, and R_{LT}) for the ^{16}O$(e,e'p)$ reaction in quasielastic kinematics at $Q^2 = 0.8$ (GeV/c)^2 and $\omega = 439$ MeV for missing energies $25 < E_{\rm miss} < 120$ MeV at various missing momenta $P_{\rm miss} \leq 340$ MeV/c. For $25 < E_{\rm miss} < 50$ MeV and $P_{\rm miss} \approx 60$ MeV/c the reaction is dominated by single-nucleon knockout from the $1s_{1/2}$-state and is described well by DWIA calculations. $(S_T - S_L)$ is smaller than that measured at $Q^2 = 0.14$ [2] and $Q^2 = 0.6$ (GeV/c)^2, but larger than that measured at $Q^2 = 1.8$ (GeV/c)^2 [11]. This is consistent with the previous observation that, at low $P_{\rm miss}$, knockout processes due to MEC and IC decrease with Q^2 [11].

At increasing missing momenta, the importance of the single-particle aspects is diminished. The cross section and the response functions no longer peak at the maximum of the s-shell (40 MeV). They no longer have the expected Lorentzian shape for s-shell knockout. DWIA calculations underestimate the cross section and response functions at $P_{\rm miss} > 200$ MeV/c by more than a factor of 10. Hence, we conclude that the single-particle aspect of the $1s_{1/2}$-state contributes less than 10% to the cross section at $P_{\rm miss} > 200$ MeV/c. This is in contrast to the p-shell case, where DWIA calculations describe the data well up to $P_{\rm miss} = 340$ MeV/c.

[3] $R_{L+TT} \equiv R_L + \frac{V_{TT}}{V_L}R_{TT}$

At $25 < E_{\rm miss} < 120$ and $P_{\rm miss} > 200$ MeV/c the cross section is almost constant in missing energy and missing momentum. For $E_{\rm miss} > 60$ MeV this feature is well reproduced by two-nucleon knockout calculations, $(e,e'pp)$ plus $(e,e'pn)$. These calculations also account for the predominantly transverse nature of the cross section, due to the large contribution from the two-body (pion exchange and isobar) currents. This indicates that the excess continuum strength at high $P_{\rm miss}$ is dominated by two body processes rather than by correlations. To our knowledge, this is the only model which can account for the shape, transversity and about the half of the magnitude of the measured continuum cross section. The unaccounted for strength suggests that additional currents and processes play an important role.

We acknowledge the outstanding support of the staff of the Accelerator and Physics Divisions at Jefferson Laboratory that made this experiment successful. We thank Dr. J. Ryckebusch for providing theoretical calculations. We also thank Dr. J.M. Udias for providing us with the NLSH bound-state wave functions. This work was supported in part by the U.S. Department of Energy contract DE-AC05-84ER40150 under which the Southeastern Universities Research Association (SURA) operates the Thomas Jefferson National Accelerator Facility, other Department of Energy contracts, the National Science Foundation, the Italian Istituto Nazionale di Fisica Nucleare (INFN), the French Atomic Energy Commission and National Center of Scientific Research, and the Natural Sciences and Engineering Research Council of Canada.

[1] J.J. Kelly, Adv. Nucl. Phys. **23**, ed. by J.W. Negele and E. Vogt, 75 (1996).
[2] P.E. Ulmer *et al.*, Phys. Rev. Lett. **59**, 2259 (1987).
[3] R. Lourie *et al.*, Phys. Rev. Lett. **56**, 2364 (1986).
[4] L. Weinstein *et al.*, Phys. Rev. Lett. **64**, 1646 (1990).
[5] J.H. Morrison *et al.*, Phys. Rev. **C59**, 221 (1999).
[6] M. Holtrop *et al.*, Phys Rev. **C58**, 3205 (1998)
[7] T. de Forest, Nucl. Phys. **A392**, 232 (1983).
[8] T. de Forest, Ann. Phys **45**, 365 (1967).
[9] J.B.J.M. Lanen *et al.*, Phys. Rev. Lett. **64**, 2250 (1990).
[10] G. van der Steenhoven *et al.*, Nucl. Phys. **A480**, 547 (1988).
[11] D. Dutta, Ph.D. thesis, Northwestern University, 1999 (unpublished).
[12] J. Ryckebusch *et al.*, Nucl. Phys. **A624**, 581 (1997).
[13] A. Gil *et al.*, Nucl. Phys. **A627**, 599 (1997).
[14] T. Takaki, Phys. Rev. **C39**, 359 (1989).
[15] A. Saha, W. Bertozzi, R.W. Lourie, and L.B. Weinstein, Jefferson Laboratory Proposal 89-003, 1989; K.G. Fissum, MIT-LNS Internal Report #02, 1997.
[16] J. Gao *et al.*, Phys. Rev. Lett. **84**, 3265 (2000).

[17] F. Garibaldi *et al.*, Nucl. Instrum. Methods **A314**, 1 (1992).
[18] www.jlab.org/Hall-A/equipment/HRS.html
[19] N. Liyanage, Ph.D. thesis, MIT, 1999 (unpublished).
[20] E. Quint, Ph.D. thesis, University of Amsterdam, 1988 (unpublished).
[21] www.physics.odu.edu/ulmer/mceep/mceep.html; see also J. A. Templon *et al.*, Phys. Rev. **C61**, 014607 (2000).
[22] E. Borie and D. Drechsel, Nucl. Phys. **A167**, 369 (1971).
[23] G. G. Simon *et al.*, Nucl. Phys. **A333**, 381 (1980); L. E. Price *et al.*, Phys. Rev. **D4**, 45 (1971).
[24] J.J. Kelly, Phys. Rev. **C60**, 044609 (1999).
[25] J. Ryckebusch *et al.*, Nucl. Phys. **A476**, 237 (1988).
[26] J. Ryckebusch *et al.*, Nucl. Phys. **A503**, 694 (1989).
[27] V. Van der Sluys *et al.*, Phys. Rev. **C55** 1982 (1997).
[28] M. Hedayati-Poor, J.I. Johansson, and H.S. Sherif, Phys. Rev. **C51**, 2044 (1995)
[29] M.M. Sharma, M.A. Nagarajan, and P. Ring, Phys. Lett. **B312**, 377 (1993).
[30] E.D. Cooper, S. Hama, B.C. Clark, and R.L. Mercer, Phys. Rev. **C47**, 297 (1993).
[31] J.P. Jeukenne and C. Mahaux, Nucl. Phys. **A394**, 445 (1983).
[32] A. Picklesimer, J. W. van Orden, and S. J. Wallace, Phys. Rev. **C32**, 1312 (1985)
[33] J. M. Udías *et al.*, Phys. Rev. Lett. **83**, 5451 (1999).
[34] S. Janssen *et al.*, **A672**, 285 (2000).

E_{beam} (GeV)	θ_e (°)	θ_{pq} (°)
0.843	100.7	0, 8, 16
1.643	37.2	0, ±8
2.442	23.4	0, ±2.5, ±8, ±16, ±20

TABLE I. Experimental Kinematics.

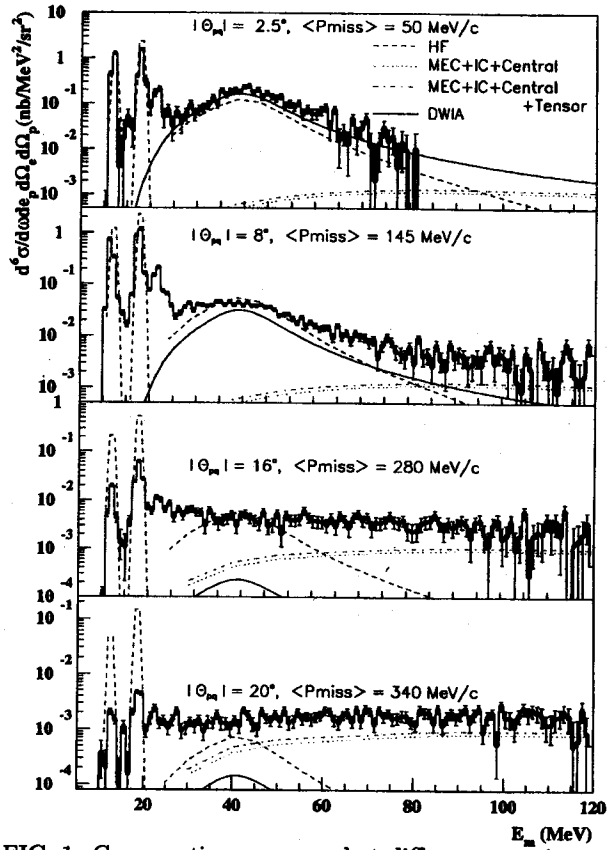

FIG. 1. Cross sections measured at different outgoing proton angles as a function of missing energy. The curves show the single-particle strength calculated by Kelly (solid curve, only s-shell is shown) and by Ryckebusch (dashed curve), folded with the Lorentzian parameterization of Mahaux. The dotted line shows the Ryckebusch *et al.* calculations of the $(e,e'pn)$ and $(e,e'pp)$ contributions to $(e,e'p)$ including meson-exchange currents (MEC), intermediate Δ creation (IC) and central correlations, while the dot-dashed line also includes tensor correlations.

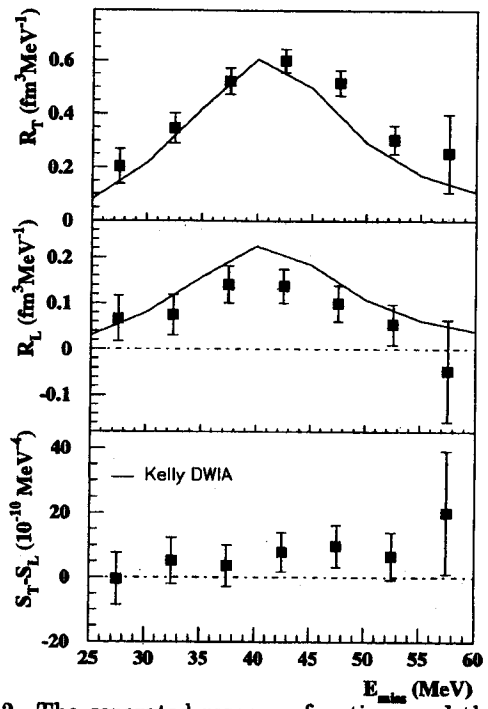

FIG. 2. The separated response functions and the difference of the longitudinal and transverse spectral functions for $\langle P_{\rm miss}\rangle \approx 60$ MeV/c. The calculations have been folded with the Lorentzian parameterization of Mahaux and have been binned in the same manner as the data.

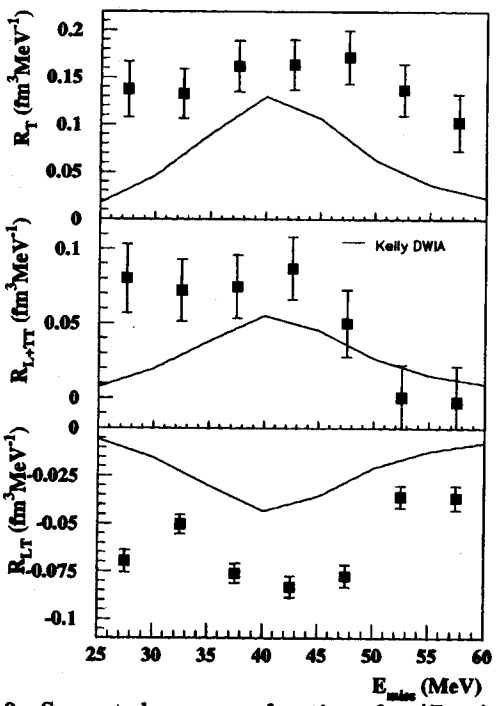

FIG. 3. Separated response functions for $\langle P_{\rm miss}\rangle \approx 145$ MeV/c.

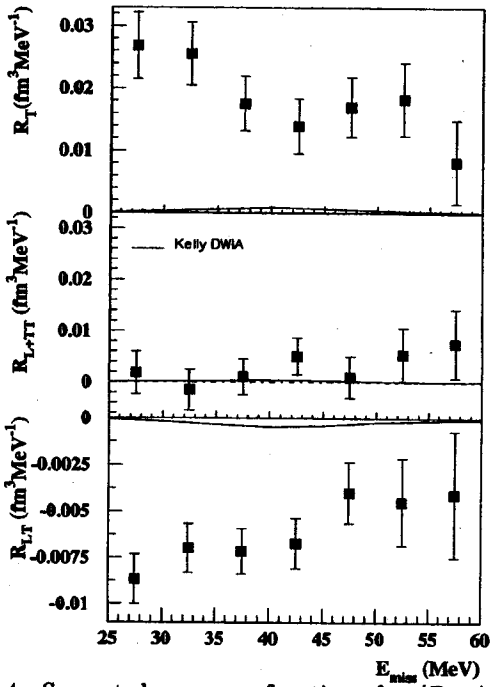

FIG. 4. Separated response functions for $\langle P_{\rm miss}\rangle \approx 280$ MeV/c.